

# Learned coupled inversion for carbon sequestration monitoring and forecasting with Fourier neural operators

Ziyi Yin, Ali Siahkoohi, Mathias Louboutin, Felix J. Herrmann  
Georgia Institute of Technology

## SUMMARY

Seismic monitoring of carbon storage sequestration is a challenging problem involving both fluid-flow physics and wave physics. Additionally, monitoring usually requires the solvers for these physics to be coupled and differentiable to effectively invert for the subsurface properties of interest. To drastically reduce the computational cost, we introduce a learned coupled inversion framework based on the wave modeling operator, rock property conversion and a proxy fluid-flow simulator. We show that we can accurately use a Fourier neural operator as a proxy for the fluid-flow simulator for a fraction of the computational cost. We demonstrate the efficacy of our proposed method by means of a synthetic experiment. Finally, our framework is extended to carbon sequestration forecasting, where we effectively use the surrogate Fourier neural operator to forecast the CO<sub>2</sub> plume in the future at near-zero additional cost.

## INTRODUCTION

Time-lapse seismic monitoring of CO<sub>2</sub> sequestration is one of the most commonly used technologies to monitor CO<sub>2</sub> dynamics in the Earth's subsurface through multiple seismic surveys (vintages) (Lumley, 2001). Time-lapse seismic has been used by carbon capture and storage (CCS) practitioners at various storage sites (Eiken et al., 2000; Arts et al., 2003; Chadwick et al., 2010; Ringrose et al., 2013; Furre et al., 2017). The growth of the CO<sub>2</sub> plumes can be inferred by time-lapse seismic imaging (Arts et al., 2003; Ayeni and Biondi, 2010; Kotsi, 2020; Yin et al., 2021) or by time-lapse full-waveform inversion (Queißer and Singh, 2013; Yang et al., 2016; Kotsi et al., 2020). Unfortunately, plain subtractions of time-lapse seismic images or inversion results often contain unwanted artifacts due to noise or to differences in acquisition (Oghenekohwo and Herrmann, 2017a; Zhou and Lumley, 2021b), which can potentially corrupt the often rather subtle time-lapse differences due to changes in CO<sub>2</sub> concentration.

Over the years, several attempts have been made to mitigate this challenge by improving the repeatability of time-lapse seismic, including the forward and backward bootstrapping method (Asnaashari et al., 2015), the double-difference method (Watanabe et al., 2004; Denli and Huang, 2009; Zhang and Huang, 2013; Yang et al., 2015), the central-difference method (Zhou and Lumley, 2021a), data assimilation via Kalman filtering (Li et al., 2014; Eikrem et al., 2019; Huang and Zhu, 2020) and the joint recovery model (Oghenekohwo et al., 2017; Wason et al., 2017; Oghenekohwo and Herrmann, 2017b; Yin et al., 2021). While these methods resulted in improvements in repeatability of time-lapse seismic, they ignore the fact that the dynamics of CO<sub>2</sub> plumes, to the leading order, adhere to two-

phase flow equations. Given physical properties of the two fluids (brine and supercritical CO<sub>2</sub>) and the spatial porosity and permeability distributions, these fluid-flow equations are capable of predicting CO<sub>2</sub> concentration snapshots during and after CO<sub>2</sub> injection. By coupling these fluid-flow equations, via a rock physics model (the patchy saturation model (Avseth et al., 2010)), to the wave equation, Li et al. (2020a) proposed an end-to-end inversion framework where time-lapse seismic surveys are jointly inverted to yield estimates for the spatial permeability distribution. Compared to the sequential inversion (Hatab and MacBeth, 2021b,a) and history matching workflows (Oliver et al., 2021), estimates of the CO<sub>2</sub> concentration in the coupled inversion are regularized by fluid-flow physics. Because coupled inversion (Li et al., 2020a) makes use of the fluid-flow equations, it offers a framework capable of producing direct estimates for the permeability. The latter can be used to generate improved predictions for the behavior of CO<sub>2</sub> plumes. Despite the initially promising results by Li et al. (2020a) on synthetic experiments, the downside of their proposed coupled framework is the increased complexity that comes with including partial differential equations (PDEs) for the fluid-flow as constraints. Aside from the need to compute sensitivities of solutions of the fluid-flow equations, solving these PDE can be computationally expensive (Settgast et al., 2018; Rasmussen et al., 2021).

To address this challenge, we propose to replace solvers for the fluid-flow PDEs by Fourier neural operators (FNOs, Li et al., 2020b). After training on a representative dataset, FNOs are capable of producing CO<sub>2</sub> plume snapshots quickly (Wen et al., 2021a; Zhang et al., 2022) while automatic differentiation (AD) gives us easy and fast access to the gradient with respect to the input. As such, trained FNOs can be considered as a data-driven surrogate for the computationally expensive fluid-flow simulations, making them a suitable candidate for the proposed coupled inversion framework that calls for multiple fluid-flow simulations including calculation of the gradient.

This extended abstract is organized as follows. First, we discuss the coupled inversion framework for seismic monitoring of geological carbon storage. Second, we introduce FNOs as surrogates for fluid-flow simulations. Next, we present the learned FNO-based coupled inversion framework where the fluid-flow solver is replaced by a pre-trained FNO. Finally, we verify the efficacy of the learned coupled inversion framework through a synthetic experiment. We further show that the trained FNO can forecast the growth of the CO<sub>2</sub> plume in the future with the inverted permeability model.

## COUPLED INVERSION FRAMEWORK

Our goal is to estimate the past, current, and future behavior of CO<sub>2</sub> plumes from available time-lapse seismic data. To

achieve this goal, we consider the coupled inversion framework proposed by Li et al. (2020a). In this framework, three types of physics are integrated, namely fluid-flow, rock, and wave physics. The CO<sub>2</sub> plume dynamics are modeled by two-phase flow equations (Pruess and Nordbotten, 2011), which we represent as the following mapping:

$$\mathbf{K} \mapsto \mathbf{c} = \mathcal{S}(\mathbf{K}) \quad \text{where } \mathbf{c} = [\mathbf{c}_1, \mathbf{c}_2, \dots, \mathbf{c}_{n_v}], \quad (1)$$

where the vectors  $\mathbf{c}_i, i = 1 \dots n_v$  are the discretized CO<sub>2</sub> concentration snapshots for each vintage. In this mapping,  $\mathcal{S}$  represents two-phase flow simulations that given the permeability,  $\mathbf{K}$ , models the CO<sub>2</sub> concentration as a spatial function over  $n_v$  consecutive times. Then, the patchy saturation model (Avseth et al., 2010) maps the  $n_v$  snapshots of the CO<sub>2</sub> concentration to seismic wavespeeds—i.e., we introduce for each vintage ( $i = 1 \dots n_v$ ) the following mapping:

$$\mathbf{c}_i \mapsto \mathbf{v}_i = \mathcal{R}(\mathbf{c}_i) \quad \text{for } i = 1, 2, \dots, n_v, \quad (2)$$

where  $\mathcal{R}$  represents the rock physics model and  $\mathbf{v}_i, i = 1 \dots n_v$  the snapshots of the acoustic wavespeed. To connect these wavespeed snapshots to the seismic data vintages, we introduce the mapping:

$$\mathbf{v}_i \mapsto \mathbf{d}_i = \mathcal{F}_i(\mathbf{v}_i) \quad \text{for } i = 1, 2, \dots, n_v, \quad (3)$$

where  $\mathcal{F}_i$  is the wave modeling operator for vintage  $i$  that generates the corresponding seismic dataset  $\mathbf{d}_i$  given the velocity model  $\mathbf{v}_i$  (Tarantola, 1984; Virieux and Operto, 2009). To arrive at the end-to-end formulation linking multi-vintage seismic data to the permeability, we finally compose (denoted by the  $\circ$  symbol) these three mappings yielding the following minimization problem:

$$\begin{aligned} & \underset{\mathbf{K}}{\text{minimize}} \quad \frac{1}{2} \|\mathcal{F} \circ \mathcal{R} \circ \mathcal{S}(\mathbf{K}) - \mathbf{d}\|_2^2 \\ & \text{where } \mathbf{d} = [\mathbf{d}_1, \mathbf{d}_2, \dots, \mathbf{d}_{n_v}], \end{aligned} \quad (4)$$

where  $\mathbf{d}$  represents the  $n_v$  vintages of the time-lapse data. While the optimization problem 4 offers a unique formulation where time-lapse seismic data are linked to the permeability, its minimization is complex since it entails nested application of the adjoint-state method (Plessix, 2006) involving computationally expensive forward simulations of both wave and fluid-flow physics. To simplify the formulation and to drastically reduce computational cost of minimization problem 4, we propose to replace the fluid-flow solves by a trained FNO.

## FOURIER NEURAL OPERATORS

There exists a growing literature on solving numerical PDEs via learned data-driven approaches involving neural networks (Lu et al., 2019; Raissi et al., 2019; Kochkov et al., 2021; Karniadakis et al., 2021). After incurring initial training costs, neural networks have been shown to provide faster alternatives to numerical PDE simulations. Recently, FNOs (Li et al., 2020b, 2021) have emerged as a powerful technique to approximate the solution operator of parametric PDEs. After training, FNOs can generate approximation solutions of PDEs from the coefficients orders of magnitude faster than numerical solvers (Li et al., 2020b). This means that computational costs, which consist

of generating training pairs coefficient (permeability  $\mathbf{K}$ ) and solution (CO<sub>2</sub> concentration  $\mathbf{c}$ ) and training the network, are sustained upfront. This front loading of computations leads to a drastic reduction in simulation time during the inversion—i.e., minimization of problem 4. We refer to the existing literature (Wen et al., 2021a; Zhang et al., 2022) for details on how to train FNOs to approximately map permeability models to the time evolution of CO<sub>2</sub> plumes. In this abstract, we assume to have  $\mathcal{S}_{\boldsymbol{\theta}}(\mathbf{K}) \approx \mathcal{S}(\mathbf{K})$  for the permeability drawn from a certain distribution. Here,  $\mathcal{S}_{\boldsymbol{\theta}}(\cdot)$  denotes the approximate map, which depends on the learned FNO weights  $\boldsymbol{\theta}$ . Given an unseen spatial distribution for the permeability  $\mathbf{K}$ , the trained FNO can instantaneously produce the time-dependant CO<sub>2</sub> concentration by forward evaluation of the FNO as  $\mathcal{S}_{\boldsymbol{\theta}}(\mathbf{K})$  (Li et al., 2020b; Wen et al., 2021a; Zhang et al., 2022). In addition, AD gives us access to the gradient with respect to FNO's input (the permeability  $\mathbf{K}$ ) that can be used for inversion. By virtue of these capabilities, the proposed approximation by FNOs can be used as a surrogate for the fluid-flow solver in the end-to-end formulation of problem 4.

## FORECAST VIA LEARNED COUPLED INVERSION

While the end-to-end formulation (shown in Figure 1) provides access to estimates of the permeability, CO<sub>2</sub> plume forecasting (Wen et al., 2021b) is our main objective because they offer guarantees that the CO<sub>2</sub> plume is progressing as planned. To meet our goal of CO<sub>2</sub> plume forecasting, the proposed learned and coupled formulation offers several distinct advantages. First, the coupled formulation uses information from all collected time-lapse vintages to arrive at estimates for the permeability itself and past and current behavior of the CO<sub>2</sub> plume. The fact that the two-phase flow equations act as a regularizer leads to improved estimates for the CO<sub>2</sub> plume (Li et al., 2020a). Second, the use of FNOs reduces the computational cost (Li et al., 2020b; Wen et al., 2021a), which potentially enables uncertainty quantification and risk management of the growth of the CO<sub>2</sub> plume in the future. Third, the coupled framework provides access to estimates for the permeability that can be used to forecast future behavior of CO<sub>2</sub> plumes. Given the estimated permeability model from the learned coupled inversion and an FNO trained on the time range of CCS projects, the current and future CO<sub>2</sub> concentration snapshots can all be generated by forward evaluation of the FNO. The forecast of CO<sub>2</sub> plume in the future can help the practitioners to detect potential failing scenarios in the early period of the CCS project, such as CO<sub>2</sub> leaking through fractures in the seal (Ringrose, 2020).

## NUMERICAL EXPERIMENTS

By means of a synthetic case study, we validate the performance of our FNO-based learned coupled inversion framework to invert for the permeability from time-lapse seismic data. We then show that we can use the estimated permeability to forecast the evolution of the CO<sub>2</sub> plume in the future. We begin by describing how we train the FNO to learn the two-phase flow

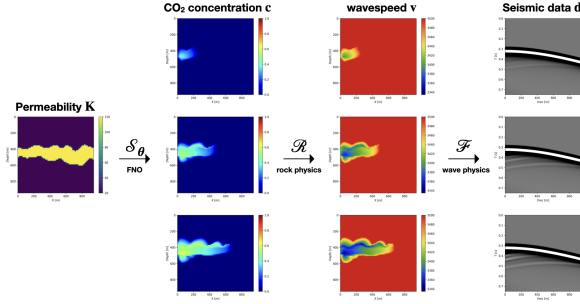


Figure 1: Learned coupled inversion framework, which contains three modules: pre-trained FNO, rock physics model, and wave physics model. Given time-lapse seismic datasets, we estimate the intrinsic permeability via end-to-end inversion.

physics.

### Training setup

We create 1000 pairs of permeability and time evolution of CO<sub>2</sub> concentration to form the training set. The size of the permeability is  $64 \times 64$  with a grid spacing of 15 m in both vertical and horizontal directions. Each permeability model is 20 millidarcies (md) everywhere except for a high permeability channel with 120 md in the central area of the model, of which the random curving boundaries are generated by a Gaussian process (Bishop and Nasrabadi, 2006). An example of the permeability model in shown in Figure 2a. For fluid-flow simulation, we add an injection well that injects supercritical CO<sub>2</sub> (with density 501.9 kg/m<sup>3</sup>) on the left-hand side of the model, and a production well that produces brine (with density 1053.0 kg/m<sup>3</sup>) on the right-hand side of the model. We assume the porosity of the reservoir is fixed to 25% homogeneously. The time evolution of the CO<sub>2</sub> concentration is modeled with [FwiFlow.jl](#) (Li et al., 2020a) over a period of 1000 days with a time step of 20 days. This numerical simulation creates 51 snapshots in total for each permeability model. We form the training dataset, where each sample is a pair of the permeability model and corresponding 51 snapshots of CO<sub>2</sub> concentration. We train an FNO that maps the input permeability  $\mathbf{K}(x, z, t)$  to the output CO<sub>2</sub> concentration  $c(x, z, t)$ . We follow the original implementation of FNOs ([https://github.com/zongyi-li/fourier\\_neural\\_operator](https://github.com/zongyi-li/fourier_neural_operator) (Li et al., 2020b) and re-implement the FNO in Julia in order to integrate with other software modules in the learned coupled inversion framework.

### Learned coupled inversion from time-lapse seismic data

After training, we show the performance of the learned coupled inversion framework described in Figure 1. During testing, we draw an unseen permeability sample, shown in Figure 2a, and generate 11 early snapshots of CO<sub>2</sub> concentration at every 40th day using the numerical solvers. The snapshots at day 40, 160 and 280 are shown in Figure 3d, 3e, 3f, respectively. Since these are the early snapshots, the CO<sub>2</sub> plume does not reach the entire high permeability channel from the left to the right. We then convert these CO<sub>2</sub> concentration snapshots to the time-varying velocity models via the patchy saturation model (Avseth et al., 2010), and generate 11 cross-well seis-

mic surveys on these 11 velocity models. The wave physics is modeled with [JUDI.jl](#) (Witte et al., 2019; Louboutin et al., 2022), which uses the highly-optimized matrix-free wave propagators of [Devito](#) (Louboutin et al., 2019; Luporini et al., 2020, 2022). Each seismic survey contains 32 active sources in a borehole on the left-hand side of the model, and 960 receivers in a borehole on the right-hand side of the model. We then invert for the permeability from the time-lapse seismic data via the learned coupled inversion framework in Figure 1. We start our initial guess as an average of the samples in the training set (a blurred channel shown in Figure 2b), and iteratively solve for the permeability by projected gradient descent with a box constraint on the permeability between 10 md and 130 md. At each iteration, we compute the seismic data misfit for only four shot records in each time-lapse survey. This reduces the cost of wave physics as only one eighth of the shot records are used during the forward and gradient evaluation (Li et al., 2012; van Leeuwen and Herrmann, 2013). We use the backtracking linear search algorithm (Stanimirović and Miladinović, 2010) to choose the step length accordingly. We use [SetIntersectionProjection.jl](#) (Peters and Herrmann, 2019; Peters et al., 2021) for box constraint projection. After 120 iterations (15 data passes on the entire time-lapse dataset), the inverted permeability is shown in Figure 2c. Since the CO<sub>2</sub> plume grows mostly at the left part of the channel (near the injection well) in these early snapshots, some part of the permeability model is in the null space thus difficult to recover exactly. However, we can see that the learned coupled inversion is able to approximately estimate the high permeability channel and to delineate curvatures especially at the upper boundary. Next, we demonstrate that this estimate is already remarkably accurate to recover the shape of the CO<sub>2</sub> plume and forecast the growth of the CO<sub>2</sub> plume in the future.

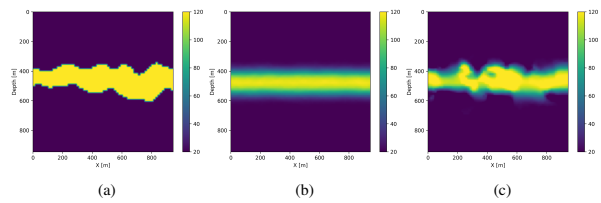


Figure 2: Learned coupled inversion from 11 seismic surveys with FNO as a surrogate. (a) Unseen ground truth permeability test sample. (b) Initial permeability. (c) Inverted permeability via 100 projected gradient descent iterations.

In addition to recovering the permeability, we are interested in CO<sub>2</sub> concentration recovery as it indicates the growing progress of the CO<sub>2</sub> plume. In Figure 3, we show the recovered CO<sub>2</sub> concentration snapshots at day 40, 160 and 280, which are acquired by a forward evaluation of FNO on the inverted permeability. We juxtapose the recovered concentrations snapshots with the ground truth and the differences for easy visualization. We observe that our predicted CO<sub>2</sub> concentration snapshots fit the ground truth accurately with very few artifacts near the boundaries of the CO<sub>2</sub> plume. This demonstrates that the proposed learned coupled inversion framework can be used successfully for carbon storage monitoring.

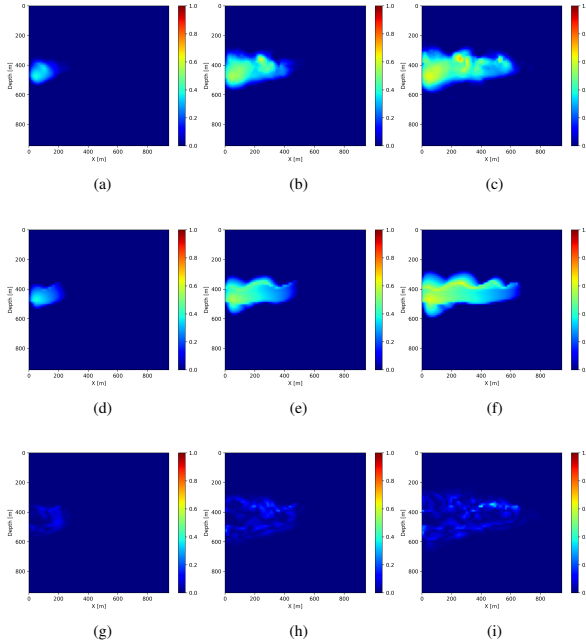


Figure 3: (a)(b)(c) Recovered snapshots of CO<sub>2</sub> concentration at 40, 160, and 280 days after injection. (d)(e)(f) Ground truth snapshots of CO<sub>2</sub> concentration. (g)(h)(i) Difference plotted in the same scale.

Finally, once we reach the 400 days, we do not have access to seismic data anymore (in the future). However, we can use the trained FNO to forecast the CO<sub>2</sub> concentration in the relatively near future assuming that the fluid dynamic will not drastically change. We show on Figure 4 the forecast at day 440, 560 and 680 by juxtaposing them with the ground truth obtained through numerical simulation and the differences. We observe that the forecast is relatively accurate and catches the global behavior of the plume even though no seismic monitoring data is available. This result confirms that the pre-trained FNO in combination with the permeability estimate from the time-lapse seismic can provide a forecasting framework for seismic monitoring of geological carbon storage.

The learned coupled inversion framework is implemented in Julia, where we use [Flux.jl](#) for AD. The scripts to reproduce the experiments are available on the SLIM GitHub page <https://github.com/slimgroup/FNO4CO2>.

## DISCUSSION AND CONCLUSION

Coupled inversion for carbon sequestration monitoring is computationally challenging as it needs to iteratively solve fluid-flow and wave equations, and differentiate through the solvers. We overcome this problem by replacing the fluid-flow solver by a pre-trained Fourier neural operator, which reduces the computational cost of fluid-flow simulations and differentiation. We demonstrated that the learned coupled inversion framework can yield reasonable estimates of the permeability of the reservoir. This estimated permeability can then be used for not only

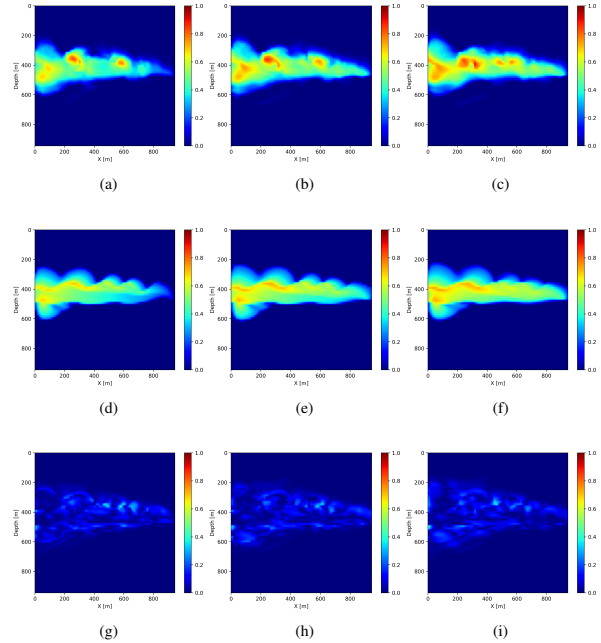


Figure 4: (a)(b)(c) CO<sub>2</sub> concentration forecast at 440, 560, and 680 days after injection. (d)(e)(f) Ground truth snapshots of CO<sub>2</sub> concentration from numerical simulation on the ground truth permeability model. (g)(h)(i) Difference plotted in the same scale.

generating the CO<sub>2</sub> concentration snapshots at the current vintages, but also forecasting the growth of the CO<sub>2</sub> plume in the future. This can potentially enable uncertainty quantification for potential plume behaviors in the future for risk management. While these initial results on learned coupled inversion are encouraging, more realistic physics phenomena can be considered in future work to numerically model the fluid-flow and wave physics more accurately. More robust inversion methods with regularization and constraints may also lead to better estimation of the permeability and CO<sub>2</sub> concentration. Future work will also involve exploration of the generalization capability of the Fourier neural operator and development of a large-scale 3D continuous monitoring framework that potentially updates the permeability according to the latest acquired seismic data from the field.

## ACKNOWLEDGEMENT

This research was carried out with the support of Georgia Research Alliance and partners of the ML4Seismic Center. The authors thank Philipp A. Witte at Microsoft for the constructive discussion.

## REFERENCES

- Arts, R., O. Eiken, A. Chadwick, P. Zweigel, L. van der Meer, and B. Zinszner, 2003, Monitoring of CO<sub>2</sub> injected at sleipner using time lapse seismic data, in J. Gale and Y. Kaya, eds., 6th International Conference on Greenhouse Gas Control Technologies: Pergamon, 347–352.
- Asnaashari, A., R. Brossier, S. Garambois, F. Audebert, P. Thore, and J. Virieux, 2015, Time-lapse seismic imaging using regularized full-waveform inversion with a prior model: Which strategy? *Geophysical Prospecting*, **63**, 78–98, doi: <https://doi.org/10.1111/1365-2478.12176>.
- Avseth, P., T. Mukerji, and G. Mavko, 2010, Quantitative seismic interpretation: Applying rock physics tools to reduce interpretation risk: Cambridge university press.
- Ayeni, G., and B. Biondi, 2010, Target-oriented joint least-squares migration/inversion of time-lapse seismic data sets: *Geophysics*, **75**, no. 3, R61–R73, doi: <https://doi.org/10.1190/1.3427635>.
- Bishop, C. M., and N. M. Nasrabadi, 2006, Pattern recognition and machine learning: Springer.
- Chadwick, A., G. Williams, N. Delepine, V. Clochard, K. Labat, S. Sturton, M. L. Buddensiek, M. Dillen, M. Nickel, A. L. Lima, and R. Arts, 2010, Quantitative analysis of time-lapse seismic monitoring data at the sleipner CO<sub>2</sub> storage operation: *The Leading Edge*, **29**, 170–177, doi: <https://doi.org/10.1190/1.3304820>.
- Denli, H., and L. Huang, 2009, Double-difference elastic waveform tomography in the time domain: 79th Annual International Meeting, SEG, Expanded Abstracts, 2302–2306, doi: <https://doi.org/10.1190/1.3255320>.
- Eiken, O., I. Breivik, R. Arts, E. Lindeberg, and K. Fagervik, 2000, Seismic monitoring of CO<sub>2</sub> injected into a marine aquifer: 70th Annual International Meeting, SEG, Expanded Abstracts, 1623–1626, doi: <https://doi.org/10.1190/1.1815725>.
- Eikrem, K. S., G. Nævdal, and M. Jakobsen, 2019, Iterated extended Kalman filter method for time-lapse seismic full-waveform inversion: *Geophysical Prospecting*, **67**, 379–394, doi: <https://doi.org/10.1111/1365-2478.12730>.
- Furre, A.-K., O. Eiken, H. Alnes, J. N. Vevatne, and A. F. Kier, 2017, 20 years of monitoring CO<sub>2</sub>-injection at Sleipner: *Energy Procedia*, **114**, 3916–3926, doi: <https://doi.org/10.1016/j.egypro.2017.03.1523>.
- Hatab, M., and C. MacBeth, 2021, Assessing data error for 4D seismic history matching: Uncertainties from processing workflow: 82nd Conference and Exhibition, EAGE, Extended Abstracts, doi: <https://doi.org/10.3997/2214-4609.202112891>.
- Hatab, M., and C. MacBeth, 2021, Assessment of data error for 4D quantitative interpretation: First International Meeting for Applied Geoscience & Energy, SEG/AAPG, Expanded Abstracts, 3439–3443, doi: <https://doi.org/10.1190/segam2021-3579836.1>.
- Huang, C., and T. Zhu, 2020, Towards real-time monitoring: Data assimilated time-lapse full waveform inversion for seismic velocity and uncertainty estimation: *Geophysical Journal International*, **223**, 811–824, doi: <https://doi.org/10.1093/gji/ggaa337>.
- Karniadakis, G. E., I. G. Kevrekidis, L. Lu, P. Perdikaris, S. Wang, and L. Yang, 2021, Physics-informed machine learning: *Nature Reviews Physics*, **3**, 422–440, doi: <https://doi.org/10.1038/s42254-021-00314-5>.
- Kochkov, D., J. A. Smith, A. Alieva, Q. Wang, M. P. Brenner, and S. Hoyer, 2021, Machine learning—accelerated computational fluid dynamics: *Proceedings of the National Academy of Sciences*, **118**, e2101784118, doi: <https://doi.org/10.1073/pnas.2101784118>.
- Kotsi, M., 2020, Time-lapse seismic imaging and uncertainty quantification: Ph. D. thesis, Memorial University of Newfoundland.
- Kotsi, M., A. Malcolm, and G. Ely, 2020, Uncertainty quantification in time-lapse seismic imaging: A full-waveform approach: *Geophysical Journal International*, **222**, 1245–1263, doi: <https://doi.org/10.1093/gji/ggaa245>.
- Li, D., K. Xu, J. M. Harris, and E. Darve, 2020, Coupled time-lapse full-waveform inversion for subsurface flow problems using intrusive automatic differentiation: *Water Resources Research*, **56**, e2019WR027032, doi: <https://doi.org/10.1029/2019WR027032>.
- Li, J. Y., S. Ambikasaran, E. F. Darve, and P. K. Kitanidis, 2014, A kalman filter powered by-matrices for quasi-continuous data assimilation problems: *Water Resources Research*, **50**, 3734–3749, doi: <https://doi.org/10.1002/2013WR014607>.
- Li, X., A. Y. Aravkin, T. van Leeuwen, and F. J. Herrmann, 2012, Fast randomized full-waveform inversion with compressive sensing: *Geophysics*, **77**, no. 3, A13–A17, doi: <https://doi.org/10.1190/geo2011-0410.1>.
- Li, Z., N. Kovachki, K. Azizzadenesheli, B. Liu, K. Bhattacharya, A. Stuart, and A. Anandkumar, 2020, Fourier neural operator for parametric partial differential equations.
- Li, Z., H. Zheng, N. Kovachki, D. Jin, H. Chen, B. Liu, K. Azizzadenesheli, and A. Anandkuma, 2021, Physics-informed neural operator for learning partial differential equations: ArXiv Preprint arxiv:2111.03794.
- Louboutin, M., M. Lange, F. Luporini, N. Kukreja, P. A. Witte, F. J. Herrmann, P. Velesko, and G. J. Gorman, 2019, Devito (v3.1.0): An embedded domain-specific language for finite differences and geophysical exploration: *Geoscientific Model Development*, **12**, 1165–1187, doi: <https://doi.org/10.5194/gmd-12-1165-2019>.
- Louboutin, M., P. Witte, Z. Yin, H. Modzelewski, and C. da Costa, 2022, Slimgroup/JUDI.jl: V2.6.4: Zenodo.
- Lu, L., P. Jin, and G. E. Karniadakis, 2019, Deeponet: Learning nonlinear operators for identifying differential equations based on the universal approximation theorem of operators: ArXiv Preprint arxiv:1910.03193.
- Lumley, D. E., 2001, Time-lapse seismic reservoir monitoring: *Geophysics*, **66**, 50–53, doi: <https://doi.org/10.1190/1.1444921>.
- Luporini, F., M. Louboutin, M. Lange, N. Kukreja, G. Bisbas, V. Pandolfo, G. Gorman, K. Hester, O. Mojica, V. Mickus, V. Leite, M. Bruno, P. Kazakas, P. Nogueira, C. Dinneen, J. H. Speglitz, G. S. von Conta, T. Greaves, I. Assis, J. F. de Souza, L. Rami, and R. Cristo, 2022, Devitocodes/devito: V4.6.2: Zenodo.
- Luporini, F., M. Louboutin, M. Lange, N. Kukreja, P. Witte, J. Hückelheim, C. Yount, P. H. J. Kelly, F. J. Herrmann, and G. J. Gorman, 2020, Architecture and performance of Devito, a system for automated stencil computation: *ACM Transactions on Mathematical Software*, **46**, 1–28, doi: <https://doi.org/10.1145/3374916>.
- Oghenekohwo, F., and F. J. Herrmann, 2017a, Highly repeatable time-lapse seismic with distributed compressive sensing—Mitigating effects of calibration errors: *The Leading Edge*, **36**, 688–694, doi: <https://doi.org/10.1190/tle36080688.1>.
- Oghenekohwo, F., and F. J. Herrmann, 2017b, Improved time-lapse data repeatability with randomized sampling and distributed compressive sensing: 79th Conference and Exhibition, EAGE, Extended Abstracts, doi: <https://doi.org/10.3997/2214-4609.201701389>.
- Oghenekohwo, F., H. Wason, E. Esser, and F. J. Herrmann, 2017, Low-cost time-lapse seismic with distributed compressive sensing—Part 1: Exploiting common information among the vintages: *Geophysics*, **82**, no. 3, P1–P13, doi: <https://doi.org/10.1190/geo2016-0076.1>.
- Oliver, D. S., K. Fossum, T. Bhakta, I. Sandø, G. Nævdal, and R. J. Lorentzen, 2021, 4D seismic history matching: *Journal of Petroleum Science and Engineering*, **207**, 109119, doi: <https://doi.org/10.1016/j.petrol.2021.109119>.
- Peters, B., and F. J. Herrmann, 2019, Algorithms and software for projections onto intersections of convex and non-convex sets with applications to inverse problems: arXiv Preprint arxiv:1902.09699.
- Peters, B., M. Louboutin, and H. Modzelewski, 2021, Slimgroup/SetIntersectionProjection.jl: V0.2.1: Zenodo.
- Plessix, R.-E., 2006, A review of the adjoint-state method for computing the gradient of a functional with geophysical applications: *Geophysical Journal International*, **167**, 495–503, doi: <https://doi.org/10.1111/j.1365-246X.2006.02978.x>.
- Pruess, K., and J. Nordbotten, 2011, Numerical simulation studies of the long-term evolution of a CO<sub>2</sub> plume in a saline aquifer with a sloping caprock: *Transport in Porous Media*, **90**, 135–151, doi: <https://doi.org/10.1007/s11242-011-9729-6>.
- Queißer, M., and S. C. Singh, 2013, Full waveform inversion in the time lapse mode applied to CO<sub>2</sub> storage at sleipner: *Geophysical Prospecting*, **61**, 537–555, doi: <https://doi.org/10.1111/j.1365-2478.2012.01072.x>.
- Raiissi, M., P. Perdikaris, and G. E. Karniadakis, 2019, Physics-informed neural networks: A deep learning framework for solving forward and inverse problems involving nonlinear partial differential equations: *Journal of Computational Physics*, **378**, 686–707, doi: <https://doi.org/10.1016/j.jcp.2018.10.045>.

- Rasmussen, A. F., T. H. Sandve, K. Bao, A. Lauser, J. Hove, B. Skaflestad, R. Klöfkorn, M. Blatt, A. B. Rustad, O. Sævareid, and K. A. Lie, 2021, The open porous media flow reservoir simulator: Computers & Mathematics with Applications, **81**, 159–185, doi: <https://doi.org/10.1016/j.camwa.2020.05.014>.
- Ringrose, P., 2020, How to store CO<sub>2</sub> underground: Insights from early-mover CCS projects: Springer.
- Ringrose, P., A. Mathieson, I. Wright, F. Selama, O. Hansen, R. Bissell, N. Saoula, and J. Midgley, 2013, The In Salah CO<sub>2</sub> storage project: Lessons learned and knowledge transfer: Energy Procedia, **37**, 6226–6236, doi: <https://doi.org/10.1016/j.egypro.2013.06.551>.
- Settgast, R. R., J. White, B. Corbett, A. Vargas, C. Sherman, P. Fu, and C. Annavarapu, 2018, Geosx simulation framework: Lawrence Livermore National Lab. (LLNL).
- Stanimirović, P. S., and M. B. Miladinović, 2010, Accelerated gradient descent methods with line search: Numerical Algorithms, **54**, 503–520, doi: <https://doi.org/10.1007/s11075-009-9350-8>.
- Tarantola, A., 1984, Inversion of seismic reflection data in the acoustic approximation: Geophysics, **49**, 1259–1266, doi: <https://doi.org/10.1190/1.1441754>.
- van Leeuwen, T., and F. J. Herrmann, 2013, Fast waveform inversion without source-encoding: Geophysical Prospecting, **61**, 10–19, doi: <https://doi.org/10.1111/j.1365-2478.2012.01096.x>.
- Virieux, J., and S. Operto, 2009, An overview of full-waveform inversion in exploration geophysics: Geophysics, **74**, no. 6, WCC1–WCC26, doi: <https://doi.org/10.1190/1.3238367>.
- Wasow, H., F. Oghenekohwo, and F. J. Herrmann, 2017, Low-cost time-lapse seismic with distributed compressive sensing—Part 2: Impact on repeatability: Geophysics, **82**, no. 3, P15–P30, doi: <https://doi.org/10.1190/geo2016-0252.1>.
- Watanabe, T., S. Shimizu, E. Asakawa, and T. Matsuoka, 2004, Differential waveform tomography for time-lapse crosswell seismic data with application to gas hydrate production monitoring: 74th Annual International Meeting, SEG, Expanded Abstracts, 2323–2326, doi: <https://doi.org/10.1190/1.1845221>.
- Wen, G., Z. Li, K. Azizzadenesheli, A. Anandkumar, and S. M. Benson, 2021a, U-FNO—An enhanced Fourier neural operator based-deep learning model for multiphase flow: arXiv Preprint arxiv:2109.03697.
- Wen, G., M. Tang, and S. M. Benson, 2021b, Towards a predictor for CO<sub>2</sub> plume migration using deep neural networks: International Journal of Greenhouse Gas Control, **105**, 103223, doi: <https://doi.org/10.1016/j.ijggc.2020.103223>.
- Witte, P. A., M. Louboutin, N. Kukreja, F. Loporini, M. Lange, G. J. Gorman, and F. J. Herrmann, 2019, A large-scale framework for symbolic implementations of seismic inversion algorithms in Julia: Geophysics, **84**, no. 3, F57–F71, doi: <https://doi.org/10.1190/geo2018-0174.1>.
- Yang, D., F. Liu, S. Morton, A. Malcolm, and M. Fehler, 2016, Time-lapse full-waveform inversion with ocean-bottom-cable data: Application on Valhall field: Geophysics, **81**, no. 4, R225–R235, doi: <https://doi.org/10.1190/geo2015-0345.1>.
- Yang, D., M. Meadows, P. Inderwiesen, J. Landa, A. Malcolm, and M. Fehler, 2015, Double-difference waveform inversion: Feasibility and robustness study with pressure data: Geophysics, **80**, no. 6, M129–M141, doi: <https://doi.org/10.1190/geo2014-0489.1>.
- Yin, Z., M. Louboutin, and F. J. Herrmann, 2021, Compressive time-lapse seismic monitoring of carbon storage and sequestration with the joint recovery model: 91st Annual International Meeting, SEG, Expanded Abstracts, 3434–3438, doi: <https://doi.org/10.1190/segam2021-3569087.1>.
- Zhang, K., Y. Zuo, H. Zhao, X. Ma, J. Gu, J. Wang, Y. Yang, C. Yao, and J. Yao, 2022, Fourier neural operator for solving subsurface oil/water two-phase flow partial differential equation: SPE Journal, 1–15.
- Zhang, Z., and L. Huang, 2013, Double-difference elastic-waveform inversion with prior information for time-lapse monitoring: Geophysics, **78**, no. 6, R259–R273, doi: <https://doi.org/10.1190/geo2012-0527.1>.
- Zhou, W., and D. Lumley, 2021a, Central-difference time-lapse 4D seismic full-waveform inversion: Geophysics, **86**, no. 2, R161–R172, doi: <https://doi.org/10.1190/geo2019-0834.1>.
- Zhou, W., and D. Lumley, 2021b, Non-repeatability effects on time-lapse 4D seismic full waveform inversion for ocean-bottom node data: Geophysics, **86**, no. 4, R547–R561, doi: <https://doi.org/10.1190/geo2020-0577.1>.